Behavioral and neural trajectories of risk taking for peer and parent in adolescence

Seh-Joo Kwon, Jessica E. Flannery, Caitlin C. Turpyn, Mitchell J. Prinstein, Kristen A. Lindquist, Eva H. Telzer*

Department of Psychology and Neuroscience, University of North Carolina at Chapel Hill
235 E. Cameron Avenue, Chapel Hill, NC, USA

* Corresponding author: Eva H. Telzer (ehtelzer@unc.edu), 235 E. Cameron Avenue, Chapel Hill, NC, USA

Abstract

One feature of adolescence is a rise in risk-taking behaviors, whereby the consequences of adolescents' risky action often impact their immediate surrounding such as their peers and parents (vicarious risk taking). Yet, little is known about how vicarious risk taking develops, particularly depending on who the risk affects and the type of risky behavior. In a 3-wave longitudinal fMRI study, 173 adolescents completed 1-3 years of a risky decision-making task where they took risks to win money for their best friend and parent (N with behavioral and fMRI data ranges from 139-144 and 100-116 participants, respectively, per wave). Results of this preregistered study suggest that adolescents did not differentially take adaptive (sensitivity to the expected value of reward during risk taking) and general (decision-making when the expected values of risk taking and staying safe are equivalent) risks for their best friend and parent from 6th to 9th grade. At the neural level, preregistered region-of-interest analyses revealed no differences in the ventral striatum and ventromedial prefrontal cortex during general nor adaptive risk taking for best friend versus parent over time. Further, exploratory longitudinal whole-brain analyses revealed sub-threshold differences between best friend and parent trajectories within regulatory regions during general vicarious risk taking and social-cognitive regions during adaptive vicarious risk taking. Our findings demonstrate that brain regions implicated in cognitive control and social-cognitive processes may distinguish behaviors involving peers and parents over time.

Keywords: adolescence, fmri, longitudinal, risk taking, social influence

Introduction

Adolescence is marked by rises in risk-taking behaviors; yet, most of adolescents' risks take place within a social context (e.g., in the presence of their peers; Chein et al., 2011). While extant research on social contextual effects on risk taking has largely focused on risks that only affect the adolescents themselves, many instances of risk taking also impact individuals around them (Do et al., 2017). For example, driving the family car and getting into an accident may result in parents' financial loss, and copying a friend's homework may result in getting the friend in trouble. In the current study, we sought to evaluate longitudinal changes in adolescents' risk taking that impacts their peers and parents, and the neural processes that support this development.

Adolescents show a remarkable ability to tune their risky behaviors to the context. For instance, adolescents take more risks for themselves than for a stranger (Crone et al., 2008), reflecting their ability to flexibly adjust their risk taking depending on who the behavior targets. Adolescents also take more risks for strangers who are perceived as "high risk-takers" than "low risk-takers" (Crone et al., 2008), demonstrating their ability to integrate others' perspectives into their decision-making process. Additionally, adolescents shift who they are willing to take risks for over time. Early adolescents take a similar amount of risks when the recipient is them or their parent (Guassi Moreira & Telzer, 2018), but young adults prioritize their parents over their peers by taking more risks to earn rewards for their parents (Guassi Moreira et al., 2018). Thus, vicarious risk taking may change between early adolescence and early adulthood, and depending on the social agent for whom the risk targets.

Rises in risk taking occur in concert with shifting patterns in adolescents' social relationships. According to social identity theory, an individual's sense of self depends on the social group to which they belong and thus their behaviors (e.g., risk behaviors) are guided by the norms (e.g., risk prototypes) espoused by their social groups (Tajfel & Turner, 1979). Family and friends are the two most salient social groups with whom adolescents identify (see Telzer et al., 2017). Across the teenage years, these relationships evolve such that adolescents become hypersensitive to peers and form interdependent friendships (Brown & Larson, 2009; Furman & Rose, 2015). Adolescents also become more independent from their parents yet also maintain intimate connections and continue to rely on their parents for guidance (Nickerson & Nagle, 2005). As a result, adolescents may take distinct risks for their peers and parents, with this difference changing over time.

Although adolescents might take risks differently for their peers and parents, the relative influence of these partners is contingent on the type of decision-making (Wilks, 1986). One common type of risk taking is adaptive risk taking, whereby an individual effectively switches between safe and risky decisions by taking advantageous risks and avoiding disadvantageous ones. Whether a risk is economically advantageous or disadvantageous relies on the expected value (EV) of the reward that is associated with risk taking. A second common type of risk taking is one's risk preferences, which may be measured by risk taking in a neutral-reward context. That is, taking risks when the EVs of risky and safe options are equivalent (and thus there is no mathematically correct decision to make) may be reflective of one's proclivity for risks. For both forms of economic risk taking, adolescents are more prone to these risks than adults, highlighting adolescence as a developmental window during which risk and reward sensitivity normatively changes (Barkley-Levenson & Galván, 2014; Paulsen et al., 2011). Given that sensitivity to social influence depends on the decision-making context, adolescents may take general (i.e., risk preferences) and adaptive (i.e., sensitivity to expected reward value) risks differently for their peers and parents over time.

Longitudinal neuroimaging methods can help us identify how neurodevelopment is associated with changes in vicarious risk taking during adolescence. In particular, adolescence is a time of a drastic reorganization of the neural systems (Nelson et al., 2005; 2016), and thus it is important to consider how the changing neural functions coincide with the changing adolescent behaviors. By contrast, some behaviors remain consistent during adolescence but these may nonetheless be paralleled by changing neural functions, suggesting that different neural strategies are needed to reach the same behavior (e.g., Eshel et al., 2007). Taking a longitudinal approach to understand the development of vicarious risky behaviors will therefore elucidate how the neurobiological strategies or demands of adolescent social behaviors, like vicarious risky behaviors, change with maturation.

Functional changes in brain regions associated with valuation (ventral stratum (VS) and ventromedial prefrontal cortex (vmPFC)) are promising neural candidates. Both animal and human neuroscience research have repeatedly identified the role of VS in reward processing (e.g., Delgado, 2007; Schultz et al., 1992). There are also developmental changes in VS functions, especially in the context of vicarious reward processing, such that there are age-related increases in the VS when processing money won for peers versus parents (Braams & Crone, 2017a). As such, the VS may subserve vicarious reward processing during risk taking for these two social agents as well. Additionally, the vmPFC has also been linked to various reward processing such as computing subjective reward values and responding to stimuli of high personal value such as close others (e.g., Bartra et al., 2008; D'Argembeau, 2013; Grabenhorst & Rolls, 2011), indicating that the vmPFC may be involved in gauging values associated with peers and parents during vicarious risk taking. These two regions are also sensitive to EV during adolescents' risk taking (Barkley-Levenson & Galván, 2014; van Duijvenvoorde et al., 2015) and are thus involved in adaptive risk taking. While the valuation system's sensitivity to EV is widely understood, it is unknown how this system tracks EV that may also hold social values. Taken together, neural patterns within the valuation system during general and adaptive risk taking may be differentially recruited for peers and parents over time.

The present preregistered study (https://osf.io/j7gsa/) utilized a longitudinal neuroimaging design to examine behavioral and neural trajectories of risk-taking behaviors that directly impact adolescents' best friend and parent. We hypothesized that at the behavioral level, adolescents will take general and adaptive risks differently for their best friend and parent across time. Similarly, we hypothesized that at the neural level, the VS and vmPFC will be differentially activated during general and adaptive risk taking for their best friend and parent across time. Given the divergent developmental trends in peer and parent influences, we did not have specific hypotheses regarding the direction of trajectories. That is, risk taking for best friend may increase faster than those for parents (Krosnick & Judd, 1982) or we may observe the opposite pattern (Cook et al., 2009). It is also possible that risk taking does not differentially change for best friend and parent across time (Chassin et al., 1986). Multivariate growth models were used to simultaneously model best friend and parent trajectories; following, post hoc contrasts tested for differences in these trajectories. We conducted *a priori* region-of-interest (ROI) analyses, supplemented with longitudinal whole-brain analyses.

Material and Methods

Participants

Adolescent participants were recruited as part of a larger study of 873 6th and 7th grade students from 3 public middle schools to participate in a longitudinal fMRI study, based on interest

and eligibility. For this current study, participants had to be at least 12 years old and in 6th or 7th grade, or within 2 months of turning 12 years old, at wave 1 of data collection. Participants were excluded if they had any metal in their body including braces or permanent retainer. Other exclusion criteria included claustrophobia, history of seizure or head trauma, learning disability, and non-fluency in English. If participants regularly took medications, they were asked to do a 24-hour medication wash prior to the scan. A total of 173 participants completed between 1-3 sessions annually across 3 waves. See Table 1 for demographic information about adolescent and parent participants. All participants were compensated for completing the session. Also, all participants provided informed consent/assent and the University's Institutional Review Board approved all aspects of the study.

In order to reach our target sample size of 150 participants after accounting for attrition and for excluded participants between waves of data collection, we recruited 2 cohorts of participants across 2 years of the study (e.g., Herd et al., 2020 for similar study design). Power analysis was performed during grant submission, which identified a target size of 150 participants (that accounts for expected attrition over the course of the study). We recruited 148 participants at wave 1 of the study (cohort 1) and 30 additional participants at wave 2 (cohort 2). Across the 3 waves, 25 participants had 1 time point of behavioral data (34 for fMRI data), 36 had 2 (39 for fMRI data), and 112 had 3 (97 for fMRI data), leading to a total of 433 behavioral and 403 fMRI data points.

At wave 1, 5 participants were excluded due to exclusionary criteria that were revealed after recruitment. These participants were not invited back for subsequent study participation. Out of the remaining 143 participants (M_{age} = 12.8, SD_{age} = 0.52; range = 11.9-14.5; 73 female), 1 participant was excluded for acute anxiety related to the fMRI scanner and 3 participants due to incomplete data (e.g., less than 60% of response on task; ending the scan early). Further, 3 participants were excluded only from the neural analyses for completing the task behaviorally (i.e., outside of the scanner), 11 participants for not having enough behavioral data or variability across trial types to be modeled at the neural level, and 9 participants for excessive motion (>0.9mm framewise displacement on >10% of total volumes). The final wave 1 sample size with behavioral and fMRI data included 139 and 116 adolescents, respectively.

At wave 2, 27 participants from cohort 1 indicated they did not want to participate or lost contact. With 30 new participants from cohort 2, 146 adolescents participated (M_{age} = 13.7; SD_{age} = 0.58; range = 12.4-15.4; 78 female). After using the same exclusionary criteria described above, the final wave 2 sample size with behavioral and fMRI data included 143 and 115 adolescents, respectively. At wave 3, 7 participants indicated they did not want to participate or lost contact and 6 participants who participated in wave 1 but skipped wave 2 returned for wave 3 of the study. As a result, 145 adolescents participated (M_{age} = 14.7; SD_{age} = 0.58; range = 13.4-16.3; 74 female). After exclusion, the final wave 3 sample size with behavioral and fMRI data included 144 and 100 adolescents, respectively. See Table 2 for more information about participants at each wave.

Procedures

At each wave of data collection, participants completed behavioral and fMRI tasks as well as self-report questionnaires, totaling a 4-hour session with a 1.5-hour fMRI session. Prior to completing the fMRI scan, participants received training for the tasks, were acclimated to a mock scanner, and completed self-report measures. In the event the participant could not participate in the fMRI session after the first wave (e.g., braces), they completed the tasks behaviorally, outside of the scanner. At the end of the session, participants received monetary compensation ($90), prizes worth up to $20 for doing well in the scan (e.g., gift cards, headphones), and a meal after

the scan. The participating parent/guardian received monetary compensation ($50), parking and gas reimbursement ($27), and a meal. At each subsequent wave, returning families received an additional $25 returning bonus (e.g., additional $25 for completing 2 waves). Adolescent participants also received additional money for themselves, their parent, and their best friend through the risky decision-making task.

Risky Decision-Making Task

Adolescents completed a modified Cups Task (Levin & Hart, 2003), which has previously been utilized to examine risky decision-making for others in developmental samples (e.g., Guassi Moreira & Telzer, 2018). Participants completed 3 runs of the Cups Task: one in which they made decisions for the self, one for parent, and one for best friend. The order in which participants completed each run was counterbalanced. Note that the self run is part of another manuscript (Kwon et al., 2021), and our focus here is on the *relative* roles of peers and parents in vicarious risky behaviors.

Each of the 3 runs consisted of 45 trials. On each trial, participants were presented with two scenarios of cups: the left side always had 1 cup with a guaranteed 15-cents hidden under the cup (Figure 1). On the right side, the number of cups (either 2, 3, or 5 cups) as well as the amount of money hidden (either 30-, 45-, or 75-cents) varied; however, the money was hidden under only one of the overturned cups. Participants were told that if they chose the right side (i.e., risky decision), then the computer would randomly select one of the cups and they may earn the higher amount or 0-cents, whereas if they chose the left side (i.e., safe decision), then they were guaranteed to earn 15-cents. After each decision, participants were shown the outcome.

On each trial, the cups were shown for 3000ms, within which participants made their decision. Next, a fixation cross was jittered around an average of 2300ms (range = 526.68-4017.12), which was followed by the outcome for 1000ms. Finally, there was an intertrial fixation cross that was jittered around an average of 2521.39ms (range = 521.14-3913.31). If participants did not make a decision within the given time, participants were told that they were “too late” and there was no change in the total points. Outcomes of each decision were added to the running total for that run, which was shown to the participant at the end of each run. At the end of each session, adolescents received the money they had earned for themselves, their parent was given the money their child had earned for them, and their best friend was provided with their earnings in cash. The participating best friend and parent did not know the adolescent was winning money for them until they received the award. For families who participated in more than one wave of data collection, 7.4% of participating parent changed at least once across their years of participation. For best friend nominations, 69.9% of adolescent participants changed their best friend at least once across their years of participation.

Operationalizing Vicarious Risk Taking

To operationalize adaptive vicarious risk taking, we assessed adolescents’ likelihood of making a risky decision as a function of the EV of reward of the risky choice. To operationalize general vicarious risk taking, we assessed adolescents’ likelihood of making a risky decision when the EVs of safe and risky choices are equal. Consistent with prior work, EV was comprised of two factors: magnitude and probability of reward, both of which contribute to taking risks when rewards are at stake (Guassi Moreira & Telzer, 2018; van Duijenvoorde et al., 2015). EV was calculated by dividing the amount of money under the cup (i.e., magnitude of reward) by the number of cups (i.e., probability of reward) for that trial. Given the parameters of the magnitudes and probabilities of reward, the EVs for risky decisions were: 6, 9, 10, 15, 22.5, 25, 37.5. The EV of safe decision was always 15. In this task, it is advantageous to take risks when the EV is greater

than 15 (i.e., EV of safe decision), whereas it is disadvantageous to take risks when the EV is less than 15. It is therefore adaptive to take risks with increasing EV.

fMRI Data Acquisition, Preprocessing, and Analysis

Imaging data were collected using a 3 Tesla Siemens Prisma MRI scanner. The Cups Task was presented on a computer screen and projected through a mirror. A high-resolution T2*-weighted echo-planar imaging (EPI) volume (TR = 2000ms; TE = 25ms; flip angle = 90°; matrix = 92 x 92; FOV = 230mm; 37 slices; slice thickness = 3mm; voxel size = 2.5 x 2.5 x 3mm^3) was acquired coplanar with a high-resolution T2*-weighted, matched-bandwidth (MBW), structural scan (TR = 5700ms; TE = 65ms; flip angle = 120°; matrix = 192 x 192; FOV = 230mm; 38 slices; slice thickness = 3mm). In addition, a T1* magnetization-prepared rapid-acquisition gradient echo (MPRAGE; TR = 2400ms; TE = 2.22ms; flip angle = 8°; matrix = 256 x 256; FOV = 256mm; 208 slices; slice thickness = 0.8mm; sagittal plane) was acquired. The orientation for the EPI and MBW scans was oblique axial to maximize brain coverage and to reduce noise.

Preprocessing was conducted using FSL (FMRIB's Software Library, version 6.0; www.fmrib.ox.ac.uk/fsl) and included the following steps: skull stripping using BET; motion correction with MCFLIRT; spatial smoothing with a 6mm Gaussian kernel, full-width-at-half maximum; high-pass temporal filtering with a 128s filter width (Gaussian-weighted least-squares straight line fitting, with sigma = 64.0s); grand-mean intensity normalization of the entire 4D dataset by a single multiplicative factor; and individual level ICA denoising for artifact signal using MELODIC (version 3.15), combined with an automated signal classifier (Tohka et al., 2008; Neyman-Pearson threshold = .3). For spatial normalization, the EPI data were registered to the T1 image with a linear transformation, followed by a white-matter boundary-based transformation using FLIRT, linear and non-linear transformations to standard Montreal Neurological Institute (MNI) 2mm brain using Advanced Neuroimaging Tools, and then spatial normalization of the EPI image to the MNI. Quality check during preprocessing and analyses ensured adequate signal coverage.

The task was modeled using an event-related design within the Statistical Parametric Mapping software package (SPM12; Wellcome Department of Cognitive Neurology, Institute of Neurology, London, UK). Individual-level fixed-effects models were created for each participant using the general linear model with regressors for the following 5 conditions: trials for each decision (risky or safe) and trials for each outcome (15-cents, zero cent, or >15-cents). A parametric modulator (PM) was included for each decision, whereby the PM represented the EV (centered at 15) of the risky decision for that trial and served to examine neural activity that tracks EV when making decisions. Each condition was modeled using the onset of the cups (or outcome) and a duration equal to zero. It was also modeled separately for each run, totaling 15 conditions. The contrasts of interest for adaptive vicarious risk taking were risky decision-making for best friend and for parent, both with EV as the PM. The contrasts of interest for general vicarious risk taking were risky decision-making for best friend and for parent, both when EV was zero (i.e., when EV of safe and risky choices are equal).

Further, trials in which participants did not respond, the final outcome trial, and volumes containing motion in excess of 0.9mm framewise displacement were included as separate regressors of no interest. Six motion regressors were modeled as covariates of non-interest to control for head movement in six dimensions. Jittered intertrial periods (i.e., fixation cross) were not explicitly modeled and therefore served as the implicit baseline for task conditions.

Regions of Interest Analyses

We used bilateral ROIs of VS and vmPFC that were defined using the Harvard-Oxford Atlas (Harvard Center for Morphometric Analysis; Figure 2). We extracted parameter estimates from the VS and vmPFC ROIs for each contrast of interest, separately for each participant at each time point. Whole-brain group-level contrasts are available on Neurovault (https://neurovault.org/collections/13322/).

Longitudinal Whole-Brain Analyses

To compliment the ROI analyses, we conducted longitudinal whole-brain analyses using AFNI 3dLMEr models (Chen et al., 2013). This program allows for voxel-level whole-brain analyses of linear mixed effects (maximum-likelihood, multi-level model). In order to assess the relative trajectories of vicarious risk taking at the whole-brain level, we modeled the interaction between risk taking for best friend versus parent and grade (for linear model; grade x grade for quadratic model) for each type of risk taking, totaling 4 models. To correct for multiple comparisons, we conducted a Monte Carlo simulation using the 3dFWHMx and 3dClustSim programs from the AFNI software package (Ward et al., 2000) and the group-level brain mask. Smoothness was estimated with the -acf option (-acf a,b,c parameters: 0.546, 4.574, 12.475), which used an average of individual-level autocorrelation function parameters that is obtained using each participant's residuals from the first-level model. This simulation indicated that a $p < .05$ Family-Wise Error corrected would be achieved with a voxel-wise threshold of $p < .001$ and a minimum cluster size of 80 voxels. The codes and outputs for longitudinal whole-brain analyses using AFNI 3dlmer are available on GitHub (https://github.com/sehjookwon/BestFriendvsParent_3dlmer).

Analysis Plan

Analysis Plan for Behavioral Trajectories of Vicarious Risk Taking

For each social target, we used a 3-level univariate growth model with trials (i = 45 trials maximum) nested within time points (j = 3 time points maximum), nested within individuals (k = 173 participants). EV that is centered at 15 was added as a level 1 predictor and grade that is centered at 6th grade as a level 2 predictor, and binary decision (0 = safe decision; 1 = risky decision) of each trial was the dependent variable (DV). We first determined the functional form that best fits the development of behavior (see below) and then added maximal random effects to the model of chosen form (Barr et al., 2013). For example, we estimated the following model to test for linear changes in behavior (lme4::glmer package in R; Bates et al., 2015):

Level 1:

$$Logit(Decision_{ijk}) = \beta_{0jk} + \beta_{1jk} EV_{ijk}$$

Level 2:

$$\beta_{0jk} = \beta_{00k} + \beta_{01k} Grade_{0jk} + u_{0jk}$$
$$\beta_{1jk} = \beta_{10k} + \beta_{11k} Grade_{1jk} + u_{1jk}$$

Level 3:

$$\beta_{00k} = \gamma_{000} + u_{00k}$$
$$\beta_{01k} = \gamma_{010} + u_{01k}$$
$$\beta_{10k} = \gamma_{100} + u_{10k}$$
$$\beta_{11k} = \gamma_{110} + u_{11k}$$

Combined Equation:

$$Logit(Decision_{ijk}) = (\gamma_{000} + \gamma_{010} Grade_{0jk}) + (\gamma_{100} EV_{ijk} + \gamma_{110} Grade_{1jk} EV_{ijk}) +$$

$$(u_{0jk} + u_{1jk} + u_{00k} + u_{01k} + u_{10k} + u_{11k})$$

Here, the first set of parentheses denotes the fixed effects of general vicarious risk taking (i.e., the average log likelihood of risky decision-making when EV is zero, which is when the EVs of safe and risky choices are equal, at 6th grade and the average trajectory of this likelihood); the second set of parentheses denotes the fixed effects of adaptive vicarious risk taking (i.e., the average log likelihood of risky decision-making as a function of EV at 6th grade and the average trajectory of this likelihood); the last set of parentheses denotes random effects of intercept, EV, and grade. From the final chosen model, we examined the effect of "intercept" and "EV" for general and adaptive vicarious risk taking, respectively, at 6th grade, and the effect of "Grade" and "Grade x EV" for grade-related changes in general and adaptive vicarious risk taking, respectively. Note, random effects were removed serially if they led to issues with random effects estimations.

Next, we conducted a multivariate growth model to evaluate how changes in risk taking for best friend relate to those for parent. For example, we estimated the following model for linear changes in behavior:

Level 1:

$$Logit(Decision_{ijk}) = BestFriend(\beta_{0jk} + \beta_{1jk}EV_{ijk}) + Parent(\beta_{0jk} + \beta_{1jk}EV_{ijk})$$

Level 2:

$$\beta_{BF0jk} = \beta_{BF00k} + \beta_{BF01k}Grade_{0jk} + u_{BF0jk}$$
$$\beta_{BF1jk} = \beta_{BF10k} + \beta_{BF11k}Grade_{1jk} + u_{BF1jk}$$
$$\beta_{Parent0jk} = \beta_{Parent00k} + \beta_{Parent01k}Grade_{0jk} + u_{Parent0jk}$$
$$\beta_{Parent1jk} = \beta_{Parent10k} + \beta_{Parent11k}Grade_{1jk} + u_{Parent1jk}$$

Level 3:

$$\beta_{BF00k} = \gamma_{BF000} + u_{BF00k}$$
$$\beta_{BF01k} = \gamma_{BF010} + u_{BF01k}$$
$$\beta_{BF10k} = \gamma_{BF100} + u_{BF10k}$$
$$\beta_{BF11k} = \gamma_{BF110} + u_{BF11k}$$
$$\beta_{Parent00k} = \gamma_{Parent000} + u_{Parent00k}$$
$$\beta_{Parent01k} = \gamma_{Parent010} + u_{Parent01k}$$
$$\beta_{Parent10k} = \gamma_{Parent100} + u_{Parent10k}$$
$$\beta_{Parent11k} = \gamma_{Parent110} + u_{Parent11k}$$

Combined Equation:

$$Logit(Decision_{ijk}) =$$
$$BestFriend(\gamma_{000} + \gamma_{010}Grade_{0jk} + \gamma_{100}EV_{ijk} + \gamma_{110}Grade_{1jk}EV_{ijk}) +$$
$$BestFriend(u_{0jk} + u_{1jk} + u_{00k} + u_{01k} + u_{10k} + u_{11k}) +$$
$$Parent(\gamma_{000} + \gamma_{010}Grade_{0jk} + \gamma_{100}EV_{ijk} + \gamma_{110}Grade_{1jk}EV_{ijk}) +$$
$$Parent(u_{0jk} + u_{1jk} + u_{00k} + u_{01k} + u_{10k} + u_{11k})$$

Here, the first and third sets of parentheses denote the fixed effects of vicarious risk taking for best friend and parent, respectively; the second and fourth sets of parentheses denote random effects of intercepts, EV, and grade for best friend and parent, respectively. Random effects were

removed serially if they led to issues with random effects estimations. To probe specific best friend versus parent effects, we then conducted post hoc tests that contrasted best friend and parent main effects (multcomp::glht package; Hothorn et al., 2008; significance level adjusted using Bonferroni correction).

Analysis Plan for Neural Trajectories of Vicarious Risk Taking

For each social target, we used a 2-level univariate growth model with time points (i) nested within individuals (j). We estimated separate models for each type of vicarious risk taking (general, adaptive) and ROI (VS, vmPFC). Parameter estimates from each ROI for each contrast of interest were the DV. Parameter estimates that were above or below 3 standard deviations from the mean (of each social target at each grade) were winsorized to 3 standard deviations to reduce the effect of extreme values. Like to the behavioral trajectory model, we first determined the best-fitting functional form and then, for example, estimated the following model to test for linear changes in neural activation (nlme::lme package; Pinheiro et al., 2022):

Level 1:

$$DV_{ij} = \beta_{0j} + \beta_{1j} Grade_{ij} + r_{ij}$$

Level 2:

$$\beta_{0j} = \gamma_{00} + u_{0j}$$
$$\beta_{1j} = \gamma_{10} + u_{1j}$$

Combined Equation:

$$DV_{ij} = \gamma_{00} + \gamma_{10} Grade_{ij} + u_{0j} + u_{1j} + r_{ij}$$

Next, for each type of vicarious risk taking and ROI, we conducted multivariate growth models to evaluate how changes in neural activations during risk taking for best friend are related to those for parent, and subsequently probed specific best friend versus parent effects. For both univariate and multivariate growth models, random effects were removed serially if they led to issues with random effects estimations. Lastly, for each type of vicarious risk taking, we conducted longitudinal whole-brain analyses using AFNI 3dLMEr models. To unpack any significant interactions and better understand the relative social influence effects at each grade, we extracted parameter estimates from each significant cluster for each contrast of interest and these estimates were then fitted into a post hoc growth model (significance level adjusted using Bonferroni correction).

Testing for Linear versus Quadratic Trajectories

For each univariate growth model above, we added a quadratic growth term: grade x grade x EV for behavioral trajectory model, grade x grade for neural trajectory models. The linear and quadratic models were formally compared using a log likelihood ratio test with difference in degrees of freedom (i.e., difference between two models in their degrees of freedom) and level of significance of $p < .05$. We also utilized Akaike's information criterion (AIC) values and Schwarz's Bayesian information criterion (BIC) for descriptive purposes. AIC and BIC values are standardized model-fit metrics, and preferred models have lower AIC and BIC values. AIC and BIC values and log likelihood ratio test results for all models are available on OSF. All models were be fit with full information maximum likelihood estimates. For neural trajectory models, each ROI was tested 6 times (2 social targets x 2 types of risks x 2 functional forms). We did not formally correct the significance level since significance was only tested on the final chosen model

and prior longitudinal fMRI studies with similar analysis procedure did not do such correction (e.g., Braams & Crone, 2017b), but this analytic decision should be considered when interpreting the results.

Deviations from Preregistration

Our current study has several deviations from our preregistration. First, we used grade instead of age as a predictor. Risk norms are often socialized, and parent and peer relationships shift in relative importance across school grades, and so vicarious risk taking may be better captured by one's social experiences (i.e., grade) than by the passage of time (i.e., age; McBride et al., 1995; O'Donnell et al., 2001). Second, we winsorized extreme values instead of entirely excluding them. Winsorizing is a method often utilized by longitudinal neuroimaging studies to reduce the influence of extreme values while retaining as much data as possible (e.g., Baranger et al., 2021; Thijssen et al., 2020). Third, we did not run our proposed VS-vmPFC functional connectivity analyses. Longitudinal changes in connectivity may vary depending on the analytic method, suggesting that changes in connectivity should be examined using a multiverse approach (Bloom et al., 2022).

Results

Behavioral Trajectories of Vicarious Risk Taking

A linear functional form best fit developmental changes in risk taking for both best friend and parent. There were no changes in general risk taking (i.e., main effect of grade on the log likelihood of making a risky decision when the EVs of risky and safe choices are equal) for best friend (γ_{Grade} = 0.065, p = 0.21) or for parent (γ_{Grade} = 0.042, p = 0.47), but there were increases in adaptive risk taking (i.e., interaction between grade and EV on the log likelihood of making a risky decision) for best friend ($\gamma_{EVxGrade}$ = 0.019, $p < 0.001$) and parent ($\gamma_{EVxGrade}$ = 0.009, p = 0.03). For best friend versus parent effects, adolescents' likelihood of taking general and adaptive risks were not significantly different between their best friend and parent at 6th grade (ps > 0.25) and across grade (ps > 0.26). Table 3 shows the predicted trajectories of each DV, R^2 values as a measure of effect size (MuMIn::r.squaredGLMM package for behavioral trajectory models and r2_nakagawa::lme4 package for neural trajectory models; Barton et al., 2009; Nakagawa et al., 2017), and multivariate analyses results.

Neural Trajectories of Vicarious Risk Taking

For ROI analyses, a linear functional form best fit developmental changes in both VS and vmPFC activation during both general and adaptive risk taking for both best friend and parent. For both best friend and parent, the VS and vmPFC did not significantly change across grade during equal-EV risk taking (i.e., general risk taking; γ_{Grade}s > -0.046, ps > 0.09) and EV tracking (i.e., adaptive risk taking; γ_{Grade}s > 0.0002, ps > 0.15). Further, there were no significant differences between best friend and parent in VS and vmPFC activation during general risk taking at 6th grade (ps > 0.2) and across grade (ps > 0.13), and during adaptive risk taking at at 6th grade (ps > 0.19) and across grade (ps > 0.44; see Table 3). Table 4 shows the mean parameter estimates of ROIs at each grade.

For longitudinal whole-brain analyses, no clusters survived the corrected cluster threshold of 80 voxels in both the linear and quadratic models of general vicarious risk taking. With a more liberal threshold ($p < 0.001$, k > 20 voxels), there were linear differences in the ventrolateral prefrontal cortex (vlPFC; x, y, z = 56, 30, 10; k = 59 voxels) and the supplementary motor area (SMA; x, y, z = 20, 4, 70; k = 53) during general risk taking for best friend versus parent across grade.

Similarly, in both the linear and quadratic models of adaptive vicarious risk taking, no clusters survived the corrected cluster threshold. With a more liberal threshold, there were linear differences in the intraparietal lobule (IPL; x, y, z = 38, -50, 46; k = 74) and quadratic differences in the cerebellum (x, y, z = -16, 66, -14; k = 48), occipital area (x, y, z = -26, -88, 24; k = 37), primary motor area (x, y, z = 0, -16, 70; k = 37) during adaptive risk taking for best friend versus parent across grade. All results should be interpreted with caution given that these clusters do not survive the corrected cluster threshold.

Secondary Analyses

Secondary Analyses: Behavioral Trajectories of Total Points Won

A linear functional form best fit developmental changes in the total points won for both best friend and parent. There were increases in the total points won for best friend (γ_{Grade} = 10.52, p = 0.048), but no changes for parent (γ_{Grade} = 2.31, p = 0.64). Adolescents did not differently win total points for their best friend and parent at 6th grade ($\gamma_{BF-Parent}$ = -4.29, p = 0.75) and across grade ($\gamma_{Grade\_BF-Grade\_Parent}$ = 3.38, p = 0.64).

Secondary Analyses: Neural Activation Collapsing Across Grade

Collapsing across grade, whole-brain analyses on general risk taking for best friend and parent both yielded activations in the VS (x, y, z = 14, 8, -4; Best friend: k = 54824, t(330) = 13.5; Parent: k = 53277, t(330) = 14.2) and the vmPFC (x, y, z = 6, 42, -14; Best friend: k = 7477, t(330) = -9.2; Parent: k = 20422, t(330) = -11.1). These whole-brain results suggest that general vicarious risk taking indeed recruits these hypothesized regions. Further, whole-brain analyses on adaptive risk taking yielded activations in the VS (Best Friend: x, y, z = -10, 8, -6, k = 68, t(330) = 4.1; Parent: x, y, z = -8, 12, -2, k = 49, t(330) = 3.5), but the vmPFC was not activated for either best friend or parent.

Secondary Analyses: Self Run

A linear functional form best fit developmental changes in behavior, neural activations, and total points won for oneself. There were no changes in general risk taking (γ_{Grade} = 0.03, p = 0.51) and total points won (γ_{Grade} = 8.49, p = 0.09), but there were increases in adaptive risk taking ($\gamma_{EVxGrade}$ = 0.019, p < .001). The vmPFC that tracked EV during risk taking marginally significantly decreased across grade (γ_{Grade} = -0.0059, p = 0.054). All other univariate growth models did not show significant grade-related effects (γ_{Grade}s > -0.0014, ps > 0.26).

Secondary Analyses: Age as a Predictor

To be consistent with our preregistered analyses, we re-ran all analyses using age instead of grade. We first winsorized extreme values to 3 standard deviations above or below the mean of each social target at each age. Adaptive risk taking for best friend (γ_{EVxAge} = 0.015, p = 0.001) increased across age, but adaptive risk taking for parent (γ_{EVxAge} = 0.006, p = 0.16) and total points won for best friend (γ_{Age} = 6.67, p = 0.18) did not change. The vmPFC that tracked EV during risk taking for best friend significantly increased across age (γ_{Age} = 0.0072, p = 0.03). All other results of univariate growth models using age were consistent with those using grade.

Discussion

The goal of this preregistered study was to investigate how behavioral and neural processing of vicarious risk taking for adolescents' close others develop. Adolescents did not take general risks (i.e., risk preferences) differently for their best friend and parent from early to mid adolescence. Though adolescents increasingly took more adaptive risks (i.e., sensitivity to expected reward value) for both their best friend and parent, the two trajectories also did not differ.

Despite the lack of behavioral differences, the adolescent brain differentially processed risks for best friend and parent during both forms of risk taking over time.

Though theory suggests there is a social reorientation away from parents and towards peers (Nelson et al., 2005; 2016), and adolescents take more risks in their peers' presence but less so in their parents' (Chein et al., 2011; Telzer et al., 2015), our behavioral findings demonstrate that peers and parents are not differentiated when risks are targeted at these two social agents. That is, peer and parent influences may differently shape youth's susceptibility to engage in risky behaviors, but not so in their ability to understand how their own risky actions have consequences on these close others. From a social identity perspective, perhaps adolescents similarly identify with their family and friend groups in vicarious risk situations, and therefore do not differentially engage in vicarious risks. In sum, these findings together identify vicarious risk taking as a unique form of socially occurring risk in adolescence.

Consistent with previous studies that demonstrate that EV sensitivity during risk taking increases across development (van Duijvenvoorde et al., 2015) but risk taking in equal-EV situations are stable across age (Levin et al., 2007), our study extends these findings to a social context. Our study shows that adolescents are more likely to take adaptive risks, but not general risks, for close others from early to mid adolescence. This result may be indicative of adolescents increasingly integrating objective contextual information, such as expected monetary reward, into their decision-making process. Thus, even in the presence of social information or under the pressure of their own risky actions having consequences on others, adolescents improve their ability to fine-tune their risky behaviors to reward information. However, though previous studies have shown *age*-related increases in non-social EV sensitivity (van Duijvenvoorde et al., 2015), our findings appear to be specific to *grade*-related increases in EV sensitivity that occur in a social context. Developmental changes in making strategic choices for close others are perhaps a socialized process, such that there are differences in such behaviors based on school-based, social experiences[1].

Longitudinal changes in the VS and vmPFC during both risk taking, however, were not different for best friend and parent. Only one other study to date has examined vicarious reward processing for best friend versus parent across adolescence (Braams & Crone, 2017a). According to this prior study, the VS was differentially activated when gaining rewards for best friend versus parent across adolescence (Braams & Crone, 2017a). By contrast, our findings posit that the VS is not differentially activated when evaluating potential reward for best friend versus parent during a decision-making process. The developmental changes in the VS's role during vicarious reward processing may therefore rely on the psychological context of the reward, such as anticipating versus receiving reward.

Lastly, we found sub-threshold linear changes in the vlPFC and SMA during general risk taking for best friend versus parent, and the IPL during adaptive risk taking. Both the vlPFC and SMA are broadly implicated in cognitive and behavioral control (Chen et al., 2010; Levy & Wagner, 2011), as well as in regulation following social feedback among adolescents (Jones et al., 2014; Masten et al., 2009). As a result, risk preferences toward close others may be subserved by differences in self-control or the need for control, with these differences shifting with grade in

[1]Another study using the same task showed that adolescents did not take adaptive risks for their parent differently over time (Kwon et al., 2021), but the said and current studies differ in how we measured adaptive risk taking. In the prior study, we extracted empirical bayes estimates to obtain a trait-like index of adaptive risk taking and this estimation shrinks individual's estimates towards the overall mean (Diez-Roux, 2002; Liu et al., 2022).

school. Further, the IPL is involved in other-oriented processes such as viewing positive social interactions and taking others' perspectives (David et al., 2006; Perino et al., 2016; van de Groep et al., 2022). Making strategic choices for close others may thus be supported by differences in attunement to close others' perspectives when decisions can benefit or harm them, with these differences again shifting with grade in school. There were also sub-threshold quadratic changes in the cerebellum, occipital area, and primary motor area, which demonstrate grade-dependent differences in the integration of sensorimotor information during thoughtful, calculated risks for close others. These results, however, do not survive corrected cluster threshold and should be interpreted with caution. Taken together, brain regions implicated in regulation during general risk taking and in social cognition during adaptive risk taking differentially process various social targets of adolescents' risky actions over time.

Our study used different types of risky behaviors, a longitudinal whole-brain method to gain a deeper understanding of neurodevelopment, and a large, diverse sample of adolescents. However, this study is not without limitations. First, peer and parent influences continue to change beyond 9th grade (Brown & Larson, 2009). Thus, it is important to investigate these trajectories across and beyond high school. Second, adolescents differentially take vicarious risks depending on the gain or loss of reward (Guassi Moreira & Telzer, 2018). Given the asymmetric development of reward and loss processing (Insel & Somerville, 2018), continued work is needed to test for differences when risks result in reward decrements for peers and parents.

Our longitudinal fMRI study investigated the developmental changes in risk taking for best friend and parent. Adolescents' heightened risky behaviors are often thought to be a byproduct of their brain processing risks and rewards in a certain way. However, neural correlates of vicarious risky behaviors are grade-dependent such that similar risky behaviors towards peers and parents are subserved by diverging neural correlates at each grade. In conclusion, adolescents may similarly identify with their peers and parents from early to mid adolescence, yet, these are modulated by diverse neural changes within this developmental window.

Data Availability Statement

The preregistration for this study is available on OSF (https://osf.io/j7gsa/). Behavioral data for this study is not publicly accessible but whole-brain group-level contrasts are available on Neurovault (https://neurovault.org/collections/13322/). The codes and outputs for longitudinal whole-brain analyses using AFNI 3dlmer are available on GitHub (https://github.com/sehjookwon/BestFriendvsParent_3dlmer).

Author Contributions

Seh-Joo Kwon: Conceptualization, Data Curation, Formal Analysis, Writing – Original Draft Preparation
Jessica E. Flannery: Formal Analysis, Writing – Review & Editing
Caitlin C. Turpyn: Formal Analysis, Writing – Review & Editing
Mitchell J. Prinstein: Conceptualization, Funding Acquisition, Writing – Review & Editing
Kristen A. Lindquist: Conceptualization, Funding Acquisition, Writing – Review & Editing
Eva H. Telzer: Conceptualization, Formal Analysis, Funding Acquisition, Writing – Original Draft Preparation

Acknowledgements

We greatly appreciate the assistance of the Biomedical Research Imaging Center at the UNC Chapel Hill, as well as members of the Developmental Social Neuroscience Lab for assistance with study design, data collection, and analysis.

Funding Information

This research was supported by the National Institutes of Health (R01DA039923 to E.H.T. and F32DA04946 to C.C.T) and the National Science Foundation (SES 1459719 to E.H.T.).

Ethical Statements

All participants were compensated for completing the session. Also, all participants provided informed consent/assent and the University's Institutional Review Board approved all aspects of the study.

References

Baranger, D., Lindenmuth, M., Nance, M., Guyer, A. E., Keenan, K., Hipwell, A. E., Shaw, D. S., & Forbes, E. E. (2021). The longitudinal stability of fMRI activation during reward processing in adolescents and young adults. *NeuroImage, 232*, 117872. https://doi.org/10.1016/j.neuroimage.2021.117872

Barkley-Levenson, E., & Galván, A. (2014). Neural representation of expected value in the adolescent brain. *Proceedings of the National Academy of Sciences of the United States of America*, *111*(4), 1646–1651. https://doi.org/10.1073/pnas.1319762111

Barton, K. (2009) MuMIn: Multi-model inference. R Package Version 0.12.2/r18. http://R-Forge.R-project.org/projects/mumin/

Bartra, O., McGuire, J. T., & Kable, J. W. (2013). The valuation system: a coordinate-based meta-analysis of BOLD fMRI experiments examining neural correlates of subjective value. *NeuroImage*, *76*, 412–427. https://doi.org/10.1016/j.neuroimage.2013.02.063

Bates, D, Mächler, M, &Bolker B, Walker, S (2015). Fitting Linear Mixed-Effects Models Using lme4. *Journal of Statistical Software*, *67*(1), 1–48. doi:10.18637/jss.v067.i01.

Bloom, P. A., VanTieghem, M., Gabard-Durnam, L., Gee, D. G., Flannery, J., Caldera, C., Goff, B., Telzer, E. H., Humphreys, K. L., Fareri, D. S., Shapiro, M., Algharazi, S., Bolger, N., Aly, M., & Tottenham, N. (2022). Age-related change in task-evoked amygdala-prefrontal circuitry: A multiverse approach with an accelerated longitudinal cohort aged 4-22 years. *Human Brain Mapping*, *43*(10), 3221–3244. https://doi.org/10.1002/hbm.25847

Braams, B. R., & Crone, E. A. (2017a). Peers and parents: a comparison between neural activation when winning for friends and mothers in adolescence. *Social Cognitive and Affective Neuroscience*, *12*(3), 417–426. https://doi.org/10.1093/scan/nsw136

Braams, B. R., & Crone, E. A. (2017b). Longitudinal Changes in Social Brain Development: Processing Outcomes for Friend and Self. *Child Development*, *88*(6), 1952–1965. https://doi.org/10.1111/cdev.12665

Brown, B. B., & Larson, J. (2009). Peer relationships in adolescence. In R. M. Lerner & L. Steinberg (Eds.), *Handbook of Adolescent Psychology: Contextual Influences on Adolescent Development* (pp. 74–103). John Wiley & Sons, Inc. https://doi.org/10.1002/9780470479193.adlpsy002004

Chassin, L., Presson, C. C., Sherman, S. J., Montello, D., & McGrew, J. (1986). Changes in peer and parent influence during adolescence: Longitudinal versus cross-sectional perspectives on smoking initiation. *Developmental Psychology*, *22*(3), 327–334. https://doi.org/10.1037/0012-1649.22.3.327

Chein, J., Albert, D., O'Brien, L., Uckert, K., & Steinberg, L. (2011). Peers increase adolescent risk taking by enhancing activity in the brain's reward circuitry. *Developmental Science*, *14*(2), F1–F10. https://doi.org/10.1111/j.1467-7687.2010.01035.x

Chen, G., Saad, Z.S., Britton, J.C., Pine, D.S., Cox, R.W. (2013). Linear mixed-effects modeling approach to FMRI group analysis. *NeuroImage*, 73, 176-190. http://dx.doi.org/10.1016/j.neuroimage.2013.01.047

Chen, X., Scangos, K. W., & Stuphorn, V. (2010). Supplementary motor area exerts proactive and reactive control of arm movements. *Journal of Neuroscience*, *30*(44), 14657–14675. https://doi.org/10.1523/JNEUROSCI.2669-10.2010

Cook, E. C., Buehler, C., & Henson, R. (2009). Peers and parents as social influences to deter antisocial behavior. *Journal of Youth and Adolescence*, *38*(9), 1240–1252. https://doi.org/10.1007/s10964-008-9348-x

Crone, E. A., Bullens, L., van Der Plas, E. A. A., Kijkuit, E. J., & Zelazo, P. D. (2008). Developmental changes and individual differences in risk and perspective taking in adolescence. *Development and Psychopathology*, *20*(4), 1213–1229. https://doi.org/10.1017/S0954579408000588

D'Argembeau A. (2013). On the role of the ventromedial prefrontal cortex in self-processing: The valuation hypothesis. *Frontiers in Human Neuroscience*, *7*, 372. https://doi.org/10.3389/fnhum.2013.00372

David, N., Bewernick, B. H., Cohen, M. X., Newen, A., Lux, S., Fink, G. R., Shah, N. J., & Vogeley, K. (2006). Neural representations of self versus other: Visual-spatial perspective taking and agency in a virtual ball-tossing game. *Journal of Cognitive Neuroscience*, *18*(6), 898–910. https://doi.org/10.1162/jocn.2006.18.6.898

Delgado M. R. (2007). Reward-related responses in the human striatum. *Annals of the New York Academy of Sciences*, *1104*, 70–88. https://doi.org/10.1196/annals.1390.002

Diez-Roux A. V. (2002). A glossary for multilevel analysis. *Journal of Epidemiology and Community Health*, *56*(8), 588–594. https://doi.org/10.1136/jech.56.8.588

Do, K. T., Guassi Moreira, J. F., & Telzer, E. H. (2017). But is helping you worth the risk? Defining Prosocial Risk Taking in adolescence. *Developmental Cognitive Neuroscience, 25*, 260–271. https://doi.org/10.1016/j.dcn.2016.11.008

Eshel, N., Nelson, E. E., Blair, R. J., Pine, D. S., & Ernst, M. (2007). Neural substrates of choice selection in adults and adolescents: development of the ventrolateral prefrontal and anterior cingulate cortices. *Neuropsychologia*, *45*(6), 1270–1279. https://doi.org/10.1016/j.neuropsychologia.2006.10.004

Furman, W., & Rose, A. J. (2015). Friendships, romantic relationships, and peer relationships. In M. E. Lamb & R. M. Lerner (Eds.), *Handbook of Child Psychology and Developmental Science: Socioemotional Processes* (pp. 932–974). John Wiley & Sons, Inc. https://doi.org/10.1002/9781118963418.childpsy322

Grabenhorst, F., & Rolls, E. T. (2011). Value, pleasure and choice in the ventral prefrontal cortex. *Trends in Cognitive Sciences*, *15*(2), 56–67. https://doi.org/10.1016/j.tics.2010.12.004

Guassi Moreira, J. F., Tashjian, S. M., Galván, A., & Silvers, J. A. (2020). Is social decision making for close others consistent across domains and within individuals? *Journal of Experimental Psychology*, *149*(8), 1509–1526. https://doi.org/10.1037/xge0000719

Guassi Moreira, J. F., & Telzer, E. H. (2018). Family conflict shapes how adolescents take risks when their family is affected. *Developmental Science*, *21*(4). https://doi.org/10.1111/desc.12611

Herd, T., King-Casas B., & Kim-Soon, J. (2020). Developmental changes in emotion regulation during adolescence: Associations with socioeconomic risk and family emotional context. *Journal of Youth and Adolescence*, *49*, 1545–1557. https://doi.org/10.1007/s10964-020-01193-2

Hothorn, T, Bretz, F, & Westfall, P (2008). Simultaneous Inference in General Parametric Models. *Biometrical Journal*, *50*(3), 346–363.

Insel, C., & Somerville, L. H. (2018). Asymmetric neural tracking of gain and loss magnitude during adolescence. *Social Cognitive and Affective Neuroscience, 13*(8), 785–796. https://doi.org/10.1093/SCAN/NSY058

Jones, R. M., Somerville, L. H., Li, J., Ruberry, E. J., Powers, A., Mehta, N., Dyke, J., & Casey, B. J. (2014). Adolescent-specific patterns of behavior and neural activity during social

reinforcement learning. *Cognitive, Affective & Behavioral Neuroscience, 14*(2), 683–697. https://doi.org/10.3758/s13415-014-0257-z

Krosnick, J. A., & Judd, C. M. (1982). Transitions in social influence at adolescence: Who induces cigarette smoking? *Developmental Psychology, 18*(3), 359–368. https://doi.org/10.1037/0012-1649.18.3.359

Kwon, S., Turpyn, C. C., Prinstein, M. J., Lindquist, K. A., & Telzer, E. H. (2021). Self-oriented neural circuitry predicts other-oriented adaptive risks in adolescence: A longitudinal study. *Social Cognitive and Affective Neuroscience*, nsab076. https://doi.org/10.1093/scan/nsab076

Levin, I. P., & Hart, S. S. (2003). Risk preferences in young children: Early evidence of individual differences in reaction to potential gains and losses. *Journal of Behavioral Decision Making, 16*(5), 397–413. https://doi.org/10.1002/bdm.453

Levin, I. P., Hart, S. S., Weller, J. A., & Harshman, L. A. (2007). Stability of choices in a risky decision-making task: A 3-year longitudinal study with children and adults. *Journal of Behavioral Decision Making, 20*(3), 241–252. https://doi.org/10.1002/bdm.552

Levy, B. J., & Wagner, A. D. (2011). Cognitive control and right ventrolateral prefrontal cortex: reflexive reorienting, motor inhibition, and action updating. *Annals of the New York Academy of Sciences, 1224*(1), 40–62. https://doi.org/10.1111/j.1749-6632.2011.05958.x

Liu, S., Kuppens, P., & Bringmann, L. (2021). On the Use of Empirical Bayes Estimates as Measures of Individual Traits. *Assessment, 28*(3), 845–857. https://doi.org/10.1177/1073191119885019

Masten, C. L., Eisenberger, N. I., Borofsky, L. A., Pfeifer, J. H., McNealy, K., Mazziotta, J. C., & Dapretto, M. (2009). Neural correlates of social exclusion during adolescence: understanding the distress of peer rejection. *Social Cognitive and Affective Neuroscience, 4*(2), 143–157. https://doi.org/10.1093/scan/nsp007

McBride, C. M., Curry, S. J., Cheadle, A., Anderman, C., Wagner, E. H., Diehr, P., & Psaty, B. (1995). School-level application of a social bonding model to adolescent risk-taking behavior. *The Journal of School Health, 65*(2), 63–68. https://doi.org/10.1111/j.1746-1561.1995.tb03347.x

Nakagawa, S., Johnson, P. C. D., & Schielzeth, H. (2017). The coefficient of determination R2 and intra-class correlation coefficient from generalized linear mixed-effects models revisited and expanded. *Journal of The Royal Society Interface, 14*(134), 20170213. doi:10.1098/rsif.2017.0213

Nelson, E. E., Jarcho, J. M., & Guyer, A. E. (2016). Social re-orientation and brain development: An expanded and updated view. *Developmental Cognitive Neuroscience, 17*, 118–127. https://doi.org/10.1016/j.dcn.2015.12.008

Nelson, E. E., Leibenluft, E., McClure, E. B., & Pine, D. S. (2005). The social re-orientation of adolescence: A neuroscience perspective on the process and its relation to psychopathology. *Psychological Medicine, 35*(2), 163–174. https://doi.org/10.1017/s0033291704003915

Nickerson, A. B., & Nagle, R. J. (2005). Peer and parent attachment in late childhood and early adolescence. *The Journal of Early Adolescence, 25*(2), 223–249. https://doi.org/10.1177/0272431604274174

O'Donnell, L., O'Donnell, C. R., & Stueve, A. (2001). Early sexual initiation and subsequent sex-related risks among urban minority youth: The reach for health study. *Family Planning Perspectives, 33*(6), 268–275.

Paulsen, D. J., Platt, M. L., Huettel, S. A., & Brannon, E. M. (2011). Decision-making under risk in children, adolescents, and young adults. *Frontiers in Psychology, 2*, 72. https://doi.org/10.3389/fpsyg.2011.00072

Perino, M. T., Miernicki, M. E., & Telzer, E. H. (2016). Letting the good times roll: Adolescence as a period of reduced inhibition to appetitive social cues. *Social Cognitive and Affective Neuroscience, 11*(11), 1762–1771. https://doi.org/10.1093/scan/nsw096

Pinheiro, J, Bates, D, & R Core Team (2022). *nlme: Linear and Nonlinear Mixed Effects Models*. R package version 3.1-160, https://CRAN.R-project.org/package=nlme.

Schultz, W., Apicella, P., Scarnati, E., & Ljungberg, T. (1992). Neuronal activity in monkey ventral striatum related to the expectation of reward. *The Journal of Neuroscience, 12*(12), 4595–4610. https://doi.org/10.1523/JNEUROSCI.12-12-04595.1992

Tajfel, H., & Turner, J. C. (1979). An integrative theory of intergroup conflict. In W., Austin & S., Worchel (Eds.), *The Social Psychology of Intergroup Relations* (pp. 33-47). Brooks/Cole.

Telzer, E. H., Ichien, N. T., & Qu, Y. (2015). Mothers know best: Redirecting adolescent reward sensitivity toward safe behavior during risk taking. *Social Cognitive and Affective Neuroscience, 10*(10), 1383–1391. https://doi.org/10.1093/scan/nsv026

Telzer, E. H., van Hoorn, J., Rogers, C. R., & Do, K. T. (2018). Social influence on positive youth development: A developmental neuroscience perspective. *Advances in Child Development and Behavior, 54*, 215–258. https://doi.org/10.1016/bs.acdb.2017.10.003

Thijssen, S., Collins, P. F., Weiss, H., & Luciana, M. (2021). The longitudinal association between externalizing behavior and frontoamygdalar resting-state functional connectivity in late adolescence and young adulthood. *Journal of Child Psychology and Psychiatry, and Allied Disciplines, 62*(7), 857–867. https://doi.org/10.1111/jcpp.13330

Tohka, J., Foerde, K., Aron, A. R., Tom, S. M., Toga, A. W., & Poldrack, R. A. (2008). Automatic independent component labeling for artifact removal in fMRI. *NeuroImage, 39*(3), 1227–1245. https://doi.org/10.1016/j.neuroimage.2007.10.013

van de Groep, S., Zanolie, K., Burke, S. M., Brandner, P., Fuligni, A. J., & Crone, E. A. (2022). Growing in generosity? The effects of giving magnitude, target, and audience on the neural signature of giving in adolescence. *Developmental Cognitive Neuroscience, 54*, 101084. https://doi.org/10.1016/j.dcn.2022.101084

van Duijvenvoorde, A. C., et al. (2015). Neural correlates of expected risks and returns in risky choice across development. *The Journal of Neuroscience, 35*(4), 1549–1560. https://doi.org/10.1523/JNEUROSCI.1924-14.2015

Ward, H. A., Riederer, S. J., Grimm, R. C., Ehman, R. L., Felmlee, J. P., & Jack, C. R. (2000). Prospective multiaxial motion correction for fMRI. *Magnetic Resonance in Medicine, 43*(3), 459–469. https://doi.org/10.1002/(sici)1522-2594(200003)43:3<459::aid-mrm19>3.0.co;2-1

Wilks, J. (1986). The relative importance of parents and friends in adolescent decision making. *Journal of Youth and Adolescence, 15*(4), 323–334. https://doi.org/10.1007/BF02145729

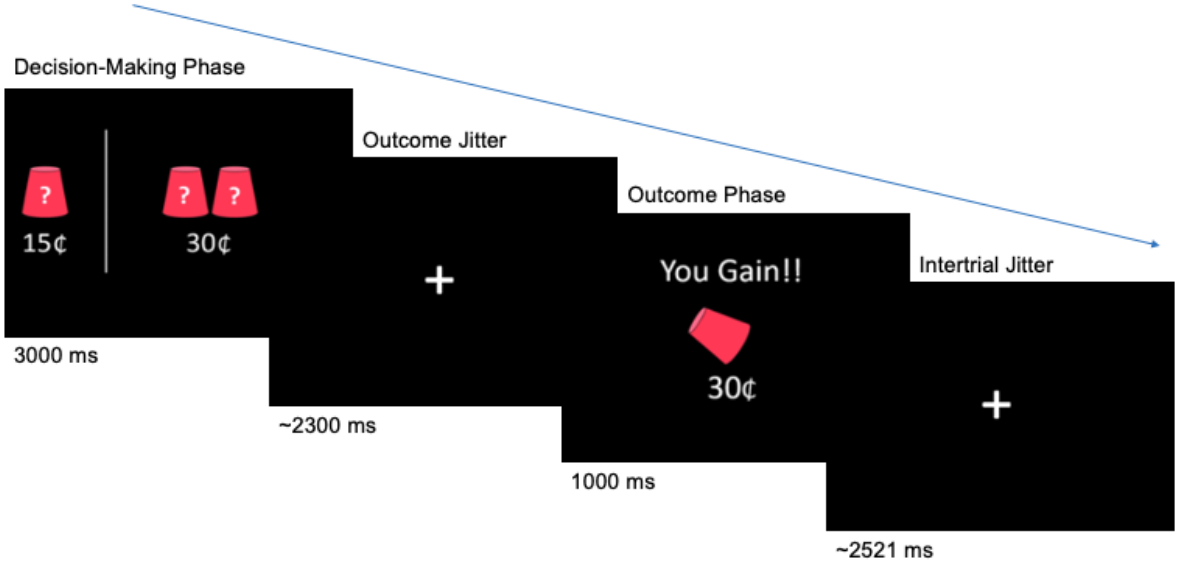

Figure 1. Example trial of the modified Cups Task. In this example, participant chose the risky option and subsequently gained a reward of 30-cents.

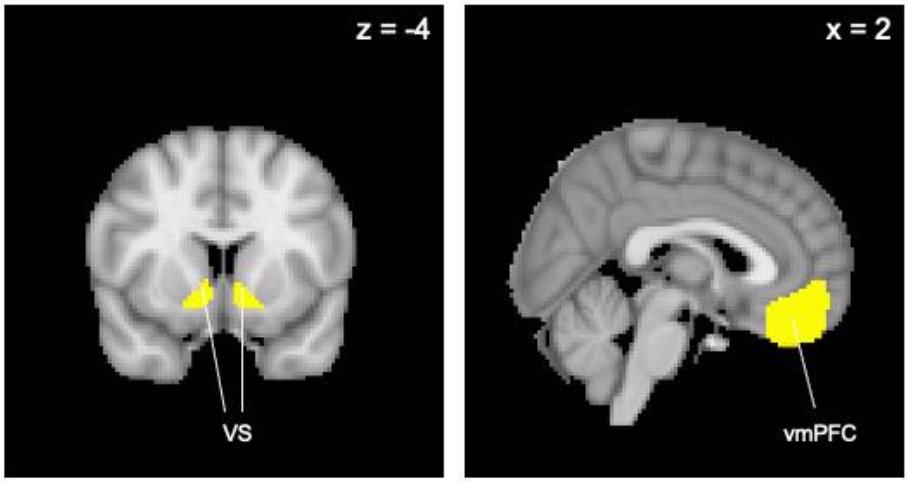

Figure 2. A priori regions of interest.

	Percentage (%)
Adolescent Participant	
Biological Sex	
Female	52.6
Male	47.4
Race	
White	29.5
Black	23.1
Hispanic/Latinx	34.7
Mixed	9.3
Other	3.5
Parent Participant	
Relationship with Adolescent Participant	
Biological mother	82.7
Biological father	9.8
Other guardian	8.1
Primary Parent Education	
Less than middle school completion	10.4
Middle school completion	3.5
Some high school	11
High school diploma	14.5
Some college	30.1
Associate's or Bachelor's degree	23.1
Some graduate school	2.3
Graduate or professional degree	5.2

Table 1. Demographic information of adolescent and parent participants at their first year of study participation.

	Wave 1	Wave 2	Wave 3
Cohort 1 / Cohort 2 sample size	143 / not yet recruited	116 / 30	119 / 26
Cohort 1 / Cohort 2 excluded for neural analyses only	23 / not yet recruited	27 / 1	40 / 4
Cohort 1 / Cohort 2 excluded for both neural and behavioral analyses	4 / not yet recruited	2 / 1	1 / 0
Final sample size for behavioral analyses	139	143	144
Final sample size for neural analyses	116	115	100
Retention rate (%)		81.1	85.3
Avg. time between waves (weeks)		49.2	52.9

Table 2. Sample size information at each wave.

	Estimate	SE	p-value	95% CI	Conditional / Marginal R2	Best Friend vs. Parent at 6th Grade / across Grades p-values
Behavioral Trajectories of General Risk Taking						
Best Friend					0.51 / 0.18	
Intercept	-0.107	0.099	0.28	[-0.301, 0.087]		
Grade	0.065	0.052	0.21	[-0.037, 0.167]		0.85 / 0.62
Parent					0.51 / 0.19	
Intercept	-0.101	0.103	0.32	[-0.303, 0.101]		
Grade	0.042	0.058	0.47	[-0.072, 0.156]		
Behavioral Trajectories of Adaptive Risk Taking						
Best Friend					0.51 / 0.18	
EV	0.091	0.011	< .001	[0.069, 0.113]		
EV x Grade	0.019	0.005	< .001	[0.009, 0.029]		0.25 / 0.26
Parent					0.51 / 0.19	
EV	0.107	0.01	< .001	[0.087, 0.127]		
EV x Grade	0.009	0.004	0.03	[0.001, 0.017]		
Neural Trajectories of General Risk Taking						
VS - Best Friend					0.17 / 0.009	
Intercept	0.268	0.094	0.005	[0.083, 0.454]		
Grade	0.094	0.055	0.09	[-0.013, 0.202]		0.2 / 0.23
VS - Parent					< 0.01 / < .001	
Intercept	0.426	0.092	< .001	[0.246, 0.606]		
Grade	0.009	0.053	0.87	[-0.095, 0.113]		
vmPFC - Best Friend					0.09 / 0.006	
Intercept	-0.689	0.104	< .001	[-0.893, -0.485]		
Grade	0.091	0.064	0.16	[-0.035, 0.216]		0.32 / 0.13
vmPFC - Parent					0.17 / 0.002	
Intercept	-0.546	0.093	< .001	[-0.729, -0.364]		
Grade	-0.046	0.06	0.44	[-0.164, 0.071]		
Neural Trajectories of Adaptive Risk Taking						
VS - Best Friend					< 0.01 / < .001	0.79 / 0.84
Intercept	0.0063	0.0048	0.19	[-0.0032, 0.0159]		

Grade	0.0002	0.0028	0.94	[-0.0053, 0.0057]		
VS - Parent					< 0.01 / < .001	
Intercept	0.0045	0.0049	0.35	[-0.005, 0.0141]		
Grade	0.001	0.0028	0.71	[-0.0045, 0.0066]		
vmPFC - Best Friend					0.1 / 0.007	
Intercept	-0.0099	0.0064	0.13	[-0.0225, 0.0028]		
Grade	0.0053	0.0036	0.15	[-0.0019, 0.0125]		0.19 / 0.44
vmPFC - Parent					0.001 / 0.001	
Intercept	0.0008	0.0053	0.89	[-0.0097, 0.0112]		
Grade	0.0016	0.0031	0.59	[-0.0044, 0.0077]		

Table 3. Best-fitting models of behavioral and neural trajectories for vicarious risk taking. Note, for behavioral trajectories of risk taking, general and adaptive risk taking were fitted in the same model.

	Grade							
	6		7		8		9	
	M	SE	M	SE	M	SE	M	SE
General Risk Taking								
VS								
Best Friend	0.243	0.116	0.337	0.074	0.563	0.084	0.481	0.112
Parent	0.420	0.127	0.449	0.066	0.416	0.082	0.479	0.095
vmPFC								
Best Friend	-0.581	0.123	-0.676	0.102	-0.394	0.085	-0.453	0.144
Parent	-0.620	0.098	-0.512	0.073	-0.677	0.087	-0.602	0.147
Adaptive Risk Taking								
VS								
Best Friend	-0.0019	0.0066	0.0113	0.0042	0.0044	0.0037	0.0055	0.0058
Parent	-0.0088	0.0068	0.0152	0.0038	-0.0001	0.0041	0.0082	0.0055
vmPFC								
Best Friend	-0.0018	0.0084	-0.0065	0.0048	-0.0015	0.0047	0.0123	0.0069
Parent	-0.0033	0.0065	0.0051	0.0047	0.0022	0.0042	0.0038	0.0066

Table 4. Parameter estimates of VS and vmPFC activation during vicarious risk taking at each grade.